

# Experimental Investigation on a Hybrid Jointed Precast Frame with Non-tearing Floor Connections.

A. Amaris, S. Pampanin, D.K. Bull & A.J. Carr

*Department of Civil Engineering, University of Canterbury, Christchurch.*



2008  
NZSEE  
Conference

**ABSTRACT:** The effects of beam elongation in concrete frame systems have demonstrated a potential source of un-expected damage to the floor systems unless adequate detailing is provided to account for displacement incompatibilities between the lateral resisting systems and the floor.

The Precast Concrete Seismic Structural Systems (PRESSSS) research program demonstrated the efficiency of dry-jointed ductile connections for moment resisting frames in order to reduce damage while sustaining high lateral loads. However, damage to precast floor systems, resulting from a geometric elongation of the beam, has yet to be addressed in detail.

Recent research carried out at University of Canterbury had proposed the concept of an innovative “non-tearing floor” jointed ductile connection solution using PRESSSS-Technology with re-centering characteristics, able to minimise the problems associated with beam elongation effects while maintaining the low-damage in the floor.

In this contribution, a series of quasi-static cyclic tests on a major 2-Dimensional, 2/3 scale, two story, single bay, precast concrete frame system with the proposed solution connection is presented.

Both experimental and analytical results confirm the unique flexibility of the proposed solution and highlight the superior performance under seismic loading sustaining only minor damage to the frame and floor systems under major earthquake events.

## 1 INTRODUCTION

Experimental and numerical studies have shown that plastic beam hinges cause growth in the beam length (Fenwick, R.C. and Fong, A., 1979, Douglas, K.T., 1992 and Fenwick, R.C. and Megget, L.M., 1993). These effects induce axial force and double bending within the beam element that not only affect the hierarchy of strength of the frames but also displacement incompatibilities which could result in the loss of support for precast floor systems due to an elongation of the beam elements. These issues should be addressed when designing the structural elements and their connections to the floor diaphragm.

Recent experimental research on the 3-dimensional behaviour of precast super-assemblages consisting of precast moment-resisting frames and precast hollowcore floor units further underlined issues related to the displacement incompatibility between precast floors and the lateral resisting system which included beam-elongation effects, although not limited to precast concrete solutions (Matthews et al., 2003). Appropriate design criteria and detailed technical solutions should thus be adopted to overcome such issues.

In the 1990's, a revolutionary alternative approach in seismic design has been developed under the PREcast Seismic Structural System (PRESSSS) Research Program coordinated by the University of California, San Diego (Priestley M.J.N., 1991, Priestley M.J.N., et al 1999). A number of beam-to-column connections and mechanical connectors, limiting the issues related to beam elongation between the precast floor units and the lateral resistant elements were developed (Priestley M.J.N.,

1996 and Nakaki, et al., 1999). The major characteristics of these connections were the use of unbonded post-tensioning techniques and grouted internal mild-steel reinforcement. During construction, the beams and columns are separated by a small gap which is subsequently grouted (Hybrid connection) or partially grouted (TCY-GAP connection). The later solution (TCY-GAP connection) was developed to avoid the primary elongation effects associated with both geometric and material beam elongation and thus the centre-to-centre distance between columns did not grow with lateral drift. However, such a solution would not account for the tearing floor actions occurring due to the gap-opening at the top of the beam.

It is worth emphasising that beam elongation effects are typical of both cast-in-situ concrete and precast concrete frames. Two contributions to beam elongation are typically recognized: a) the material contribution due to the cumulative residual strain within the steel, and b) the geometrical contribution due to the presence of a neutral axis and actual depth of the beam. With regards to jointed ductile connections with re-centering characteristics, the extent of beam elongation is significantly reduced, being limited to the geometrical contribution alone. Furthermore, such effects could be minimized when a reduced depth of the beam is adopted due to the use of internal prestressing or external post-tensioning.

## **2 REDUCING DAMAGE IN THE FLOOR**

Towards to reduce damage in the floor different approaches had been found in the literature. First one based on a rocking frame system using traditional jointed (herein called gapping) ductile connection (e.g PRESSS technology) in combination with an articulated (jointed) floor. The Second approach had been recently developed for frame systems (non-gapping systems) with a standard floor solution (i.e. topping and continuous starter bars).

### **2.1 Gapping frames systems**

A number of mechanical connections between double-tee floor diaphragms to perform under in-plane seismic forces were developed under the PRESSS research program (Priestley M.J.N., 1996). A welded X-plate mechanical connector (Fig. 1-left) between the double-tee floor members and the frame beams was implemented for the PRESSS five-storey precast concrete test building with a satisfactory results although significant inelastic actions and permanent distortion were reported (Priestley M.J.N., et al 1999).

Recent investigation on different alternative behaviour of double-tee flange connectors subjected to in-plane monotonic and reversed cyclic loads had been performed (Pincheira et al., 2005). Experimental evidence indicates that strength, stiffness, and deformation capacity are highly dependant on the constraint and load condition.

Based on previous work carried out in the PRESSS program (Priestley et al., 1999) and recent research carried out at the University of Canterbury (Pampanin et al., 2006), was developed for traditional hybrid technology. The precast hollow-core floor systems were connected to the lateral resisting system by means of appropriately located (or deformation compatible) mechanical couplers.

The solution relies upon a double hinge mechanism at the beam-column interface (used as a shear key transfer mechanism) and on sliding shear keys in the horizontal plane used as connectors between frame and floor system. As a result, the system is able to accommodate the displacement incompatibility between floor and frame by creating an articulated or jointed mechanism effectively decoupled in the two directions (Fig. 1-right). According to the proposed solution, the hollowcore unit is in fact connected to the lateral beams by shear mechanical connectors acting as shear keys when the floor moves (relatively) in the direction orthogonal to the beam and as sliders when the floor moves in the direction parallel to the beam. Results of this research showed that beam elongation effects (in this case limited to the geometrical contribution) can be avoided by using a traditional gapping solution and a smart floor-frame connection. No damage in the floor system due to the gap opening mechanism are thus expected. Also, due to the low flexural stiffness of the shear keys-connectors in the out of plane directions, torsion of the beam elements due to pull out of the floor or relative rotation of floor

and edge support, can be limited.

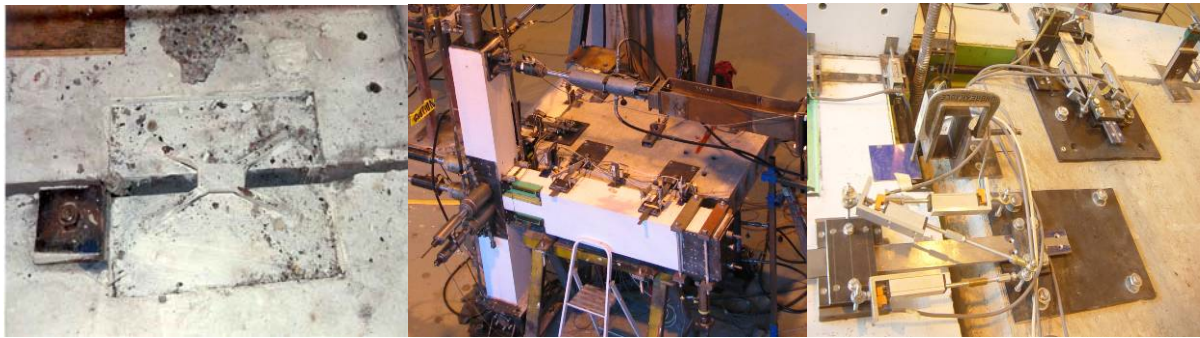


**Figure 1. PRESSSS X-plate mechanical connector type (left) and beam-column joint with articulated floor unit: Overall view (centre) and connection details (right).**

## 2.2 Non-gapping frame systems

Experimental research in emulated cast-in-situ beam column joint subassemblies had demonstrated to minimize the damage of the floor using the “slotted beam concept” where the beam is constructed with a narrow vertical slot at the beam ends that runs from the bottom of the beam up to the bottom of the floor (Ohkubo, M and Hamamoto, T., 2004). The system is govern by the flexural strength of the bottom beam reinforcement which is continuous through the slot, meanwhile yielding of the top reinforcement is avoided and minor beam elongation effects are generated.

Using two different beam-column connections implemented in the PRESSSS research the program (Priestley et al., 1999), had shown the feasibility of implementing a non-tearing-floor seismic resisting system, while still relying on more traditional floor-to-frame connections (i.e. topping and continuous starter bars) herein called non-gapping frame systems (Amaris et al., 2007).

One of the connections called the Hybrid frame connection (Figure 2-left) used unbonded post-tensioning through the centre of the joint which acts as a clamping force with self-centring properties and the use of mild-steel reinforcement inside ducts and grouted for bond conditions.

Another innovative beam-column connection called the Tension-Compression Yield-GAP solution (TCY GAP) (Figure 2-centre) was introduced using top mild-steel bars inserted into grouted sleeves and the use of unbonded post-tension tendons at the bottom of the beam. The peculiarity of this system was that beams and columns were separated by a small gap partially grouted to avoid the primary elongation effects, thus not affecting the centre-to-centre distance between columns. However, such a solution would not account for the tearing floor actions occurring due to the gap-opening at the top of the beam. Furthermore, no re-centering contribution was provided by the tendons located with a straight profile in the centre of the compression grout.

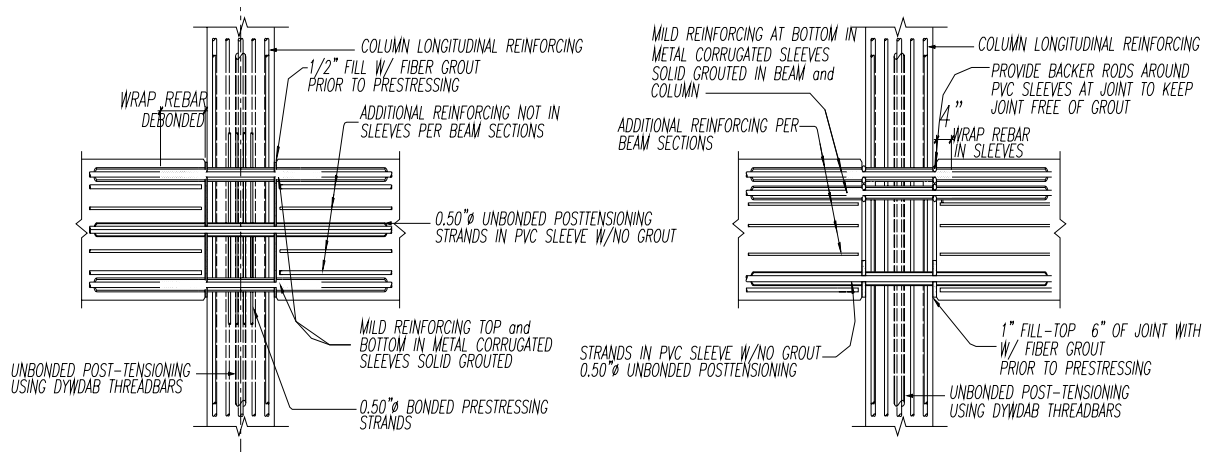


**Figure 2. Hybrid beam-to-column connections: Hybrid PRESSSS(left),TCY-GAP(right)**

The evolution of the connection started from an inverted TCY-Gap solution (Fig. 3- left), based on a single top hinge (top pad or similar contact thick element) with a gap and grouted internal mild steel bars in the bottom part of the beam. This modification prevents both elongation and tearing effects in the floor whilst no-recentring capacities can be provided due to the location and straight profile of the tendons.

A further conceptual evolution using a single top-hinge mechanism, an antisymmetric profile of the unbonded post-tensioned tendons and external mild-steel dissipation devices was introduced (Fig. 3-right). The connection inherently minimises the problems associated with beam elongation effects while also providing a global system re-centring and minimising damage to the hybrid connection.

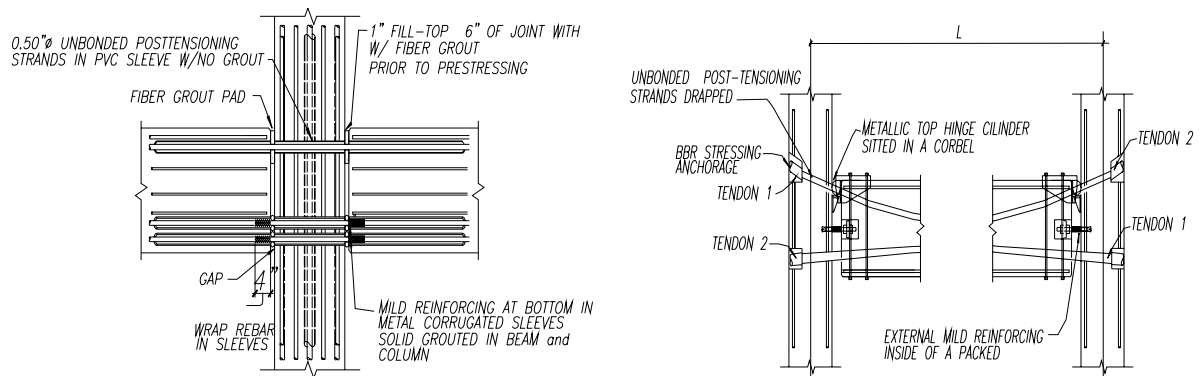


**Figure 3. Evolution of the Hybrid systems: Inverted TCY-GAP (left) and Hybrid Frame with draped unbonded tendons and metallic top hinge (right)**

Very satisfactory results were obtained through experimental quasi-static cyclic testing on 2/3 scaled beam-column joint sub-assemblies, implementing the proposed non-tearing floor solution (Amaris et al., 2007). However, the full re-centering properties of the subassembly could not be appreciated due to the use of a straight tendon configuration as well as of a single beam-column connection solution.

In this contribution in order to demonstrate the advantages of having the non-tearing-floor seismic resisting frames and the global re-centring contribution, a series of large scale tests on a 2-Dimensional two-storey, one-bay precast frame super-assemblage are presented along with analytical-experimental comparisons.

### 3 EXPERIMENTAL TESTING OF A TWO-STORY FRAME WITH AN ALTERNATIVE NON-TEARING CONNECTION

In the following paragraphs, an up-to-date summary of recent results is outlined. An extensive experimental research programme is ongoing at the University of Canterbury on the development of an innovative floor-to-lateral-load-resisting, “non-tearing floor” connection.

A precast concrete prototype building consists of a six storey, five bays by four bays was developed as part of the experimental and analytical work. The prototype structure was designed following a direct displacement based design (DDBD) procedure (Priestley, 2002). After distributing the base shear, the internal actions were scaled to respect similitude requirements for the test specimen. However, due to the space and capacity limitations within the structural laboratory, the test structure does not totally represent the prototype building. The test specimen is considered more as a “non-tearing-floor” proof of concept, which is the main objective of the experimental programme.

The proof of concept test specimen was constructed with prototype beam and column dimensions and with a design beam moment of 190kNm. The columns carried a total axial load of 160kN which represents the tributary axial floor loads acting on each column for a two storey frame.

### 3.1 Test set-up and specimen description

The experimental test set-up of the 2/3 scale, two dimensional, two-storey one-bay precast frame is shown in Figure 4. The precast frame system consists of one bay at 6.86m in length between the column centrelines and two storeys at 2.06m and 2.10m in height for the first and second floor respectively. Precast beams and columns were designed according to the New Zealand Concrete Structures Standard NZ3101:2006.

The precast beams are composed of a rectangular section of 470x300mm. An I-shape section was designed at the beam ends to accommodate hidden energy dissipaters. A 500mm square column cross section was adopted. External column end Stubs of 600x250mm at the beam column joint were used on both sides of the joint to reduce steel congestion and allow for a more efficient distribution of compression stresses for the post-tensioned joint.

A total of eight 7-wire prestressing strands were used within each beam ( $A_{pt,total} = 792\text{mm}^2$ ), requiring four tendons in each of the two ducts per beam. This resulted in the required design beam moment of 180kNm at 2% of lateral drift. An initial post-tensioning force of 50% of the ultimate stress  $f_{ptu}$  (1860MPa) was applied to each set of four strands, thus equivalent to an initial post-tensioning force of approximately 372kN.

Axial force was applied to the columns via four unbonded post-tensioned tendons ( $A_{pt} = 396\text{mm}^2$ ) for each column (one tendon in each single duct) as illustrated in Figure 4. An initial post-tensioning force at 22% of the ultimate stress  $f_{ptu}$  (1860MPa) was applied, thus equivalent to an initial post-tensioning force of approximately 162kN for each column.

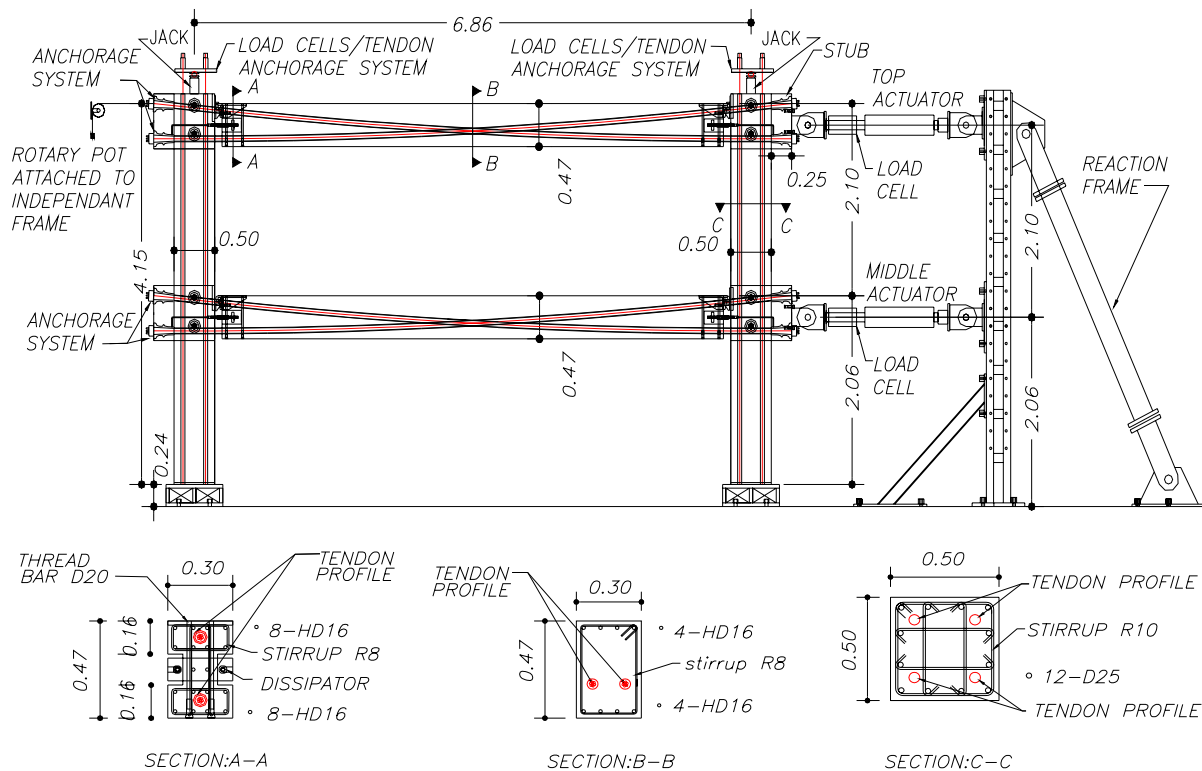


Figure 4. Test set up and specimen description.

### 3.2 Loading history

A series of quasi-static cyclic displacement control tests were carried out under increasing levels of lateral top displacement, where the structure was displacement controlled for the top floor and force controlled for the first floor: this ensured the correct lateral load distribution between the two levels. The testing protocol complied with the “acceptance criteria” proposed in (ACI T1.1-01 & ACI T1.1R-01 2001) and consisted of a series of three cycles of drift, followed by a smaller single cycle.

### 3.3 Testing program

During the imposed displacement protocol, a rocking mechanism was developed at the column base. Two variations on testing were considered, 1) maintaining a constant column axial load or 2) varying the column axial load. Furthermore, three dissipation contents were considered for each axial load regime above to demonstrate the re-centring capabilities of the frame.

In the first case, a constant load representing the gravity load of 162kN in each column was applied and maintained during testing to the unbonded post-tensioned tendons achieved by a release valve within the hydraulic jack system (Fig. 4).

In the second case, the post-tensioned tendons were locked off resulting in an increase to the column axial load due to the elongation of the post-tensioned tendons as the columns rocked upon their foundation. In normal construction practice, these tendon forces may have initial post-tensioned forces in addition to the gravity contribution. However, in this experimental programme the initial post-tensioned forces were assumed to equal the gravity load of 162kN. This test parameter was chosen to limit the demands imposed to the strong floor within the Civil Engineering Laboratory.

Table 1 summarises the entire test program where the column axial load is represented by either constant (PT) or variable (PT<sub>NC</sub>), while 7, 10 and 13 denotes the diameter of the mild steel dissipater.

**Table 1. Test Summary.**

Test	Column Axial Load Type	Dissipation Type
PT <sub>NC</sub>	Not constant	Post-tensioned only solution
PT	Constant	Post-tensioned only solution
PT <sub>NC</sub> 7	Not constant	7mm fuse
PT7	Constant	7mm fuse
PT <sub>NC</sub> 10	Not constant	10mm fuse
PT10	Constant	10mm fuse
PT <sub>NC</sub> 10	Not constant	13mm fuse

### 3.4 Connection details

The connection detail (Fig. 5-left) comprises of a steel mono-hinge and armouring at the beam ends and a hidden corbel (acting as the beam-shear transfer mechanism). A T-shaped steel section is used to prevent beam uplift and torsion. An asymmetric unbonded post-tensioned tendon profile is adopted and combined with external energy dissipaters for supplementary damping.

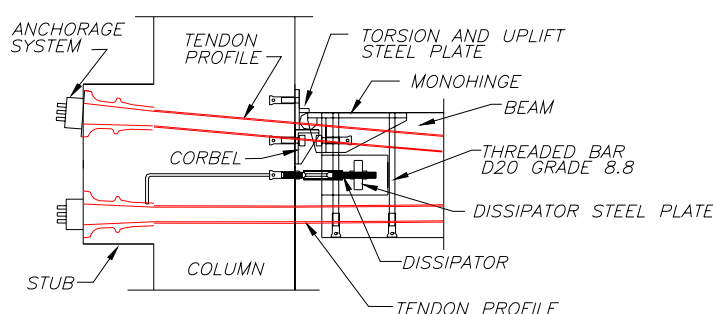


**Figure 5. Connection detail.**

**Mono-hinge:** A steel armour was cast into the concrete during construction of the beams which consist of three steel plates (one top and two lateral) welded together. A steel cylinder (with one quarter removed) was connected to the top of the steel plate and welded to the steel armouring. The steel hinge element is attached to the beam using four high strength threaded bars bolted to the top

steel plate and threaded into the underside of the beam.

**Corbel:** The corbel consists on a steel angle, stiffened with four welded steel plates which added to the shear and bending capacity of the corbel. The steel corbel was attached to the column using high strength bolts, threaded into cast in-situ inserts.

**Torsion, uplift and construction tolerances:** The T-shape steel section (located directly above the steel cylinder) was located at both ends of the beam (Fig. 5-left) to prevent torsion, beam uplift and tolerance issues. Uplifting occurs due to the vertical component of the post-tensioned forces (static case) and due to the laterally induced beam shear. Torsion is induced in the beams via two effects. The first is that the top and bottom tendon profiles are separated in plan at mid-span, introducing a plan eccentricity. This effect creates torsion in beam that could be significant. The second torsion effect can occur when the precast floor units sit on the beam with an eccentricity - the vertical forces (dead load) are not applied in the centre of the beam, this induces additional torsion into the beam.

Construction tolerances were considered in the following manner:

- Product tolerances were considered for the precast beam by making them 20mm shorter in length than required. Steel shims were used to make up these tolerances and to transmit the axial compression forces from the beam to the column.
- Erection tolerances were the same as the tolerances that will occur in normal construction process.

**Mild steel dissipater fuse and steel plate:** An important component for hybrid solutions are the external energy dissipaters used as supplemental damping devices. The objective of adding external energy dissipation is to dissipate the earthquake-induced energy via sacrificial elements that can easily replaced after a strong earthquake. This minimises costs associated with repair and downtime when compared to conventional buildings.

The mild steel dissipater (Fig. 6) is fabricated from round mild steel bar, threaded at each end and machined down to a specific bar diameter over a pre-determined length; defined as the unbonded length. The unbonded length prevents premature fracture of the bar by limiting the strains to allowable limits. A 34mm (outside diameter) steel tube with a wall thickness of 2mm (anti-buckling restraint), is located over the machined area of the steel bar and temporary fixed in place. Epoxy was then injected into a hole supplied at the bottom of the steel confinement tube to ensure that all the air was expelled out from the top.

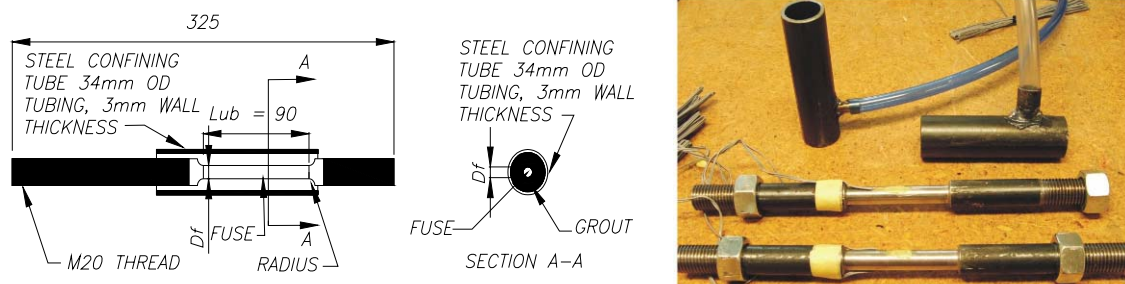


**Figure 6. Dissipators rods detail.**

Three different fuse diameters ( $D_f$ ) were considered: 7mm, 10mm and 13mm with an unbonded length of 90mm. The device was designed to ensure all the plastic deformation is confined to the fused region of the steel bar.

The dissipaters are expected to be displaced in net tension and compression displacements due to the specific nature of the mono-hinge connection. Cyclic tests reveal that the dissipater has a reduced energy dissipation capacity when displaced into net negative displacements, promoted further by buckling at relatively low displacements.

Figure 7 (left) presents the experimental cyclic and monotonic tests of the 7mm diameter fused

dissipater. It can be seen that larger dissipater forces are induced when the dissipater is displaced into net compression. Figure 7 (right) illustrates the mechanics of the dissipater as it comes into contact with the surrounding epoxy when displaced in compression, increasing the stiffness and strength of the element. Depending on the relative capacity of the dissipater, failure can occur either by the dissipater yielding in compression or the epoxy crushing in compression.

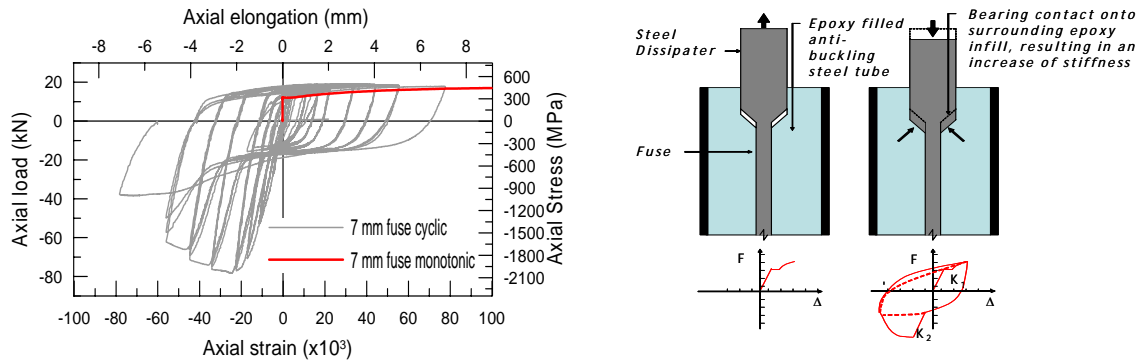


Figure 7. Cyclic and monotonic dissipater test (left) and behaviour in compression (right).

## 4 TEST FRAME EXPERIMENTAL RESPONSE

### 4.1 Behaviour of Unbonded Post-Tensioned-only Solution

Two tests were first carried out on an unbonded post-tensioned only solution: a) varying the column axial load (test  $PT_{NC}$ ) or b) having a constant axial load (test  $PT$ ). Figure 8 shows the force displacement hysteretic behaviour up to 3.5% drift for the post-tensioned solution having varying axial load. In general the behaviour was a stable non linear elastic response with some dissipation coming from friction within the ducts and within the steel mono-hinge. No significant reduction in stiffness on loading was observed.

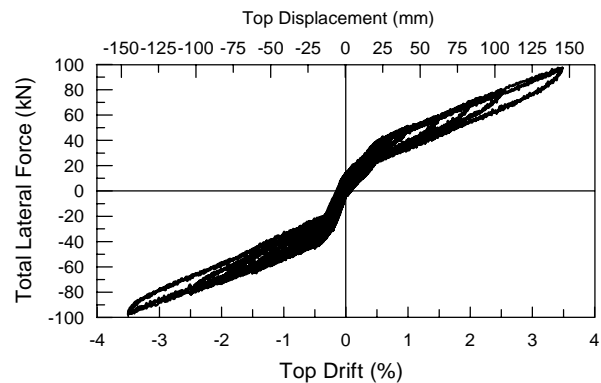
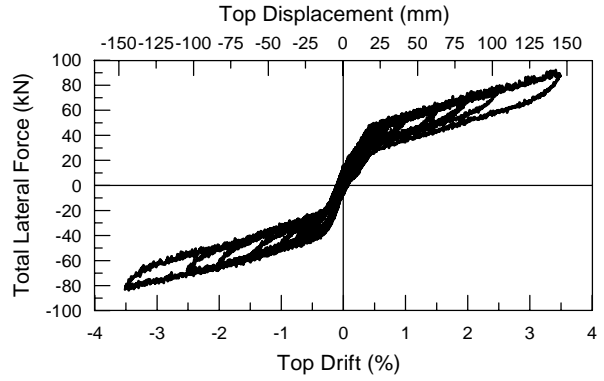


Figure 8. Unbonded post-tensioned only solution for test  $PT_{NC}$  : global hysteresis loop at 3.5 % drift.

Similar behaviour was observed for the constant axial load, post-tensioned solution test  $PT$  (Figure 9). An increment in the energy dissipation was observed when compared to test  $PT_{NC}$  due to additional friction forces being introduced into the system as a result of the setup controlling the axial load during testing.





**Figure 9. Unbonded post-tensioned only solution for test PT: global hysteresis loop at 3.5 % drift.**

A larger bi-linear stiffness is observed for test  $PT_{NC}$  when compared to test PT due to the increment in axial load increasing the column moment and thus the lateral capacity.

The column axial load behaviour for test  $PT_{NC}$  and test PT is shown in Figure 10 left and right respectively. When the gap opens at the column base, the additional tendon elongation provides additional axial load for test  $PT_{NC}$  (Figure 10-left).

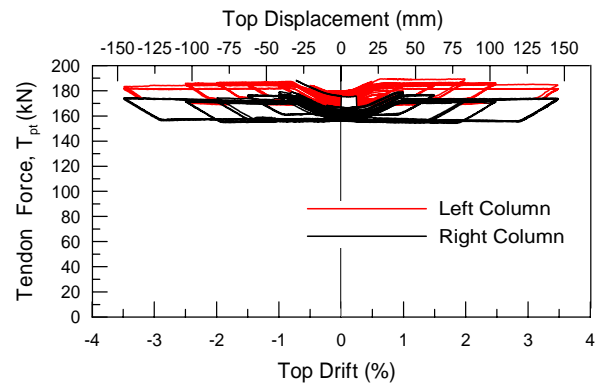
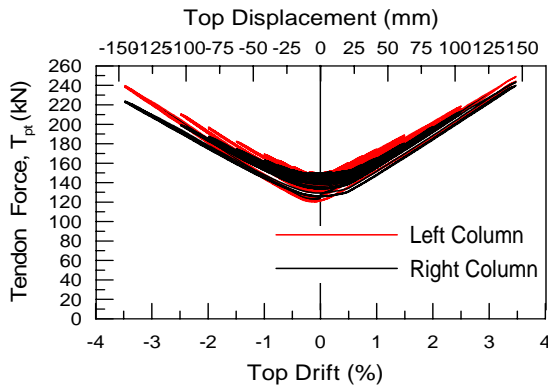


**Figure 10. Behaviour of the post-tensioned tendons in the columns: test  $PT_{NC}$  (left) and test PT (right).**

Figure 10 (right) shows axial load variations of  $\pm 10$  kN for test PT due to the accuracy of the axial load control system.

The column to foundation moment versus base rotation is illustrated in Figure 11 for tests  $PT_{NC}$  and PT. As expected, an increase in the moment is observed for test  $PT_{NC}$  (Fig 11-left) due to the increment in tendon force, while a constant moment rotation response is observed for test PT in Figure 11 (right).

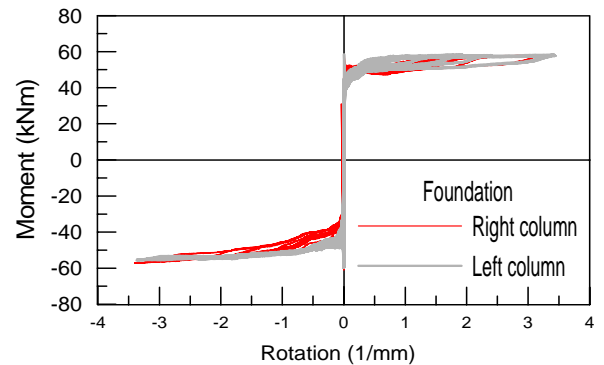
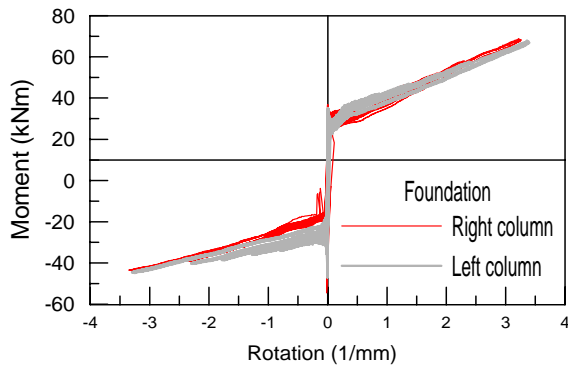


**Figure 11. Moment-rotation behaviour in the foundation: test  $PT_{NC}$  (left) and test PT (right).**

It should be noted that such a system does not necessarily require full static re-centring in order to have zero (or near zero) permanent deformations following an earthquake. In fact, the natural dynamic re-centring due to the small cycle hysteretic behaviour following the major excursions during the earthquake can be sufficient to restore the entire system to the original position after the free oscillations. It is worth emphasising that while a majority of the re-centring is being provided by the columns, an allowance for column gravity loads and additional post-tensioned tendons within the columns can be used to achieve a full static re-centring solution combined with the benefits of a non-tearing floor system.

In terms of local responses, Figure 12 shows the gap opening response at the top and bottom of the beam depth. Maximum gap displacements of 1.3 mm (top) and 16 mm (bottom) were obtained at a lateral drift of 3.5%.

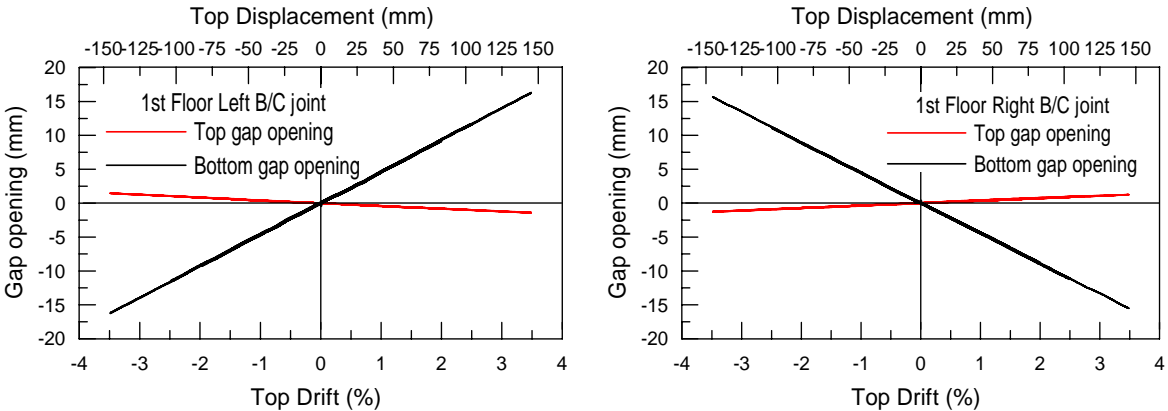


Figure 12. Gap opening of the B/C Joint at 3.5% of drift.

Considering that the neutral axis position remains constant at any drift level, a simple calculation can be used to determine the moment demand in the joint, while the forces in the tendons can be determined from geometry which remain elastic (Fig. 13-left).

Figure 13 (right) shows the moment versus rotation response of the beam-column connection. As expected, a linear elastic behaviour is observed with an initial moment of 150 kNm due to the initial post-tensioned force of the tendons. Adopting a positive convention for moments (anti-clockwise direction) the moment at the left and right beam column connection are self-equilibrated in each floor at zero drift. For a positive joint rotation (gap opening), the left moment capacity increases while the right moment decreases in the same proportion due to the asymmetric tendon profiles.

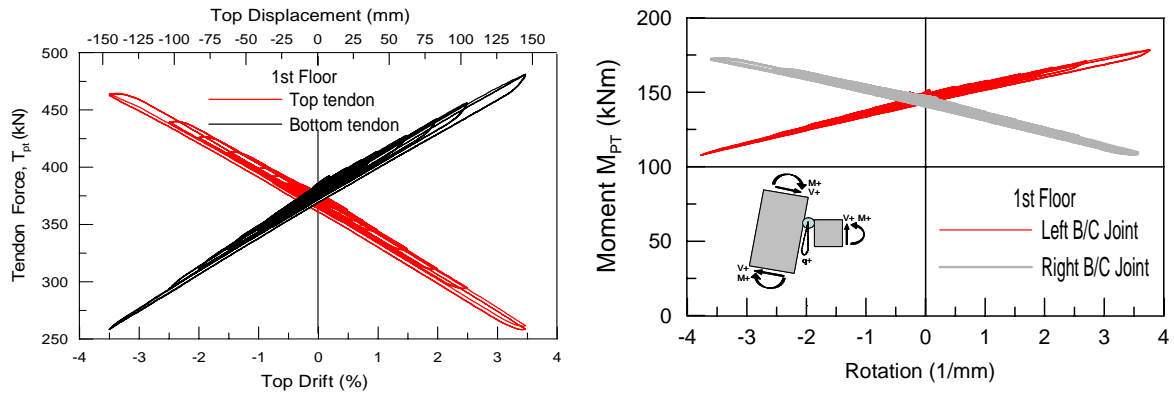


Figure 13. Beam post-tensioned forces (left) and B/C joint moment rotation behaviour (right).

#### 4.2 Behaviour of the Hybrid Solution

Additional energy dissipation capability was added to the unbonded post-tensioned only solution in the form of mild steel external dissipaters. As per testing reported above, the same series of tests and test set-up were carried out for the hybrid solution.

The experimental results presented in Figure 14 correspond to the force displacement hysteresis behaviour of test PT<sub>NC</sub>7 (7 mm fuse dissipaters, variable axial load). A stable flag shape hysteresis is observed with higher dissipation when compared to the unbonded post-tensioned only solution. Furthermore, re-centring is achieved up to a lateral drift of 3.5%. The concave bilinear slope indicates the onset of stiffness degradation as a result of buckling of the external dissipaters in compression.

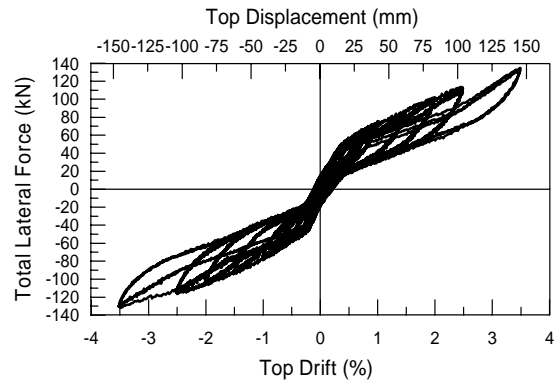
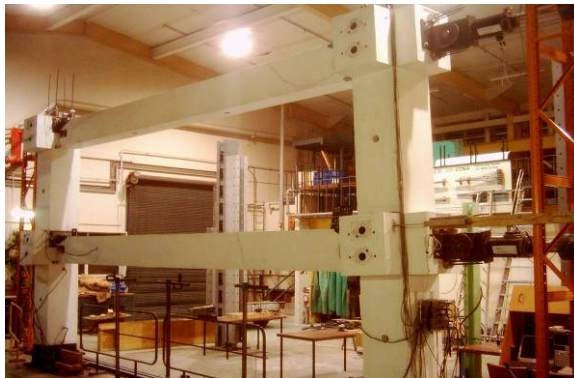


Figure 14. Hybrid system with external dissipaters for TEST PT<sub>NC</sub>7: global hysteresis loop at 3.5 % drift.

A similar force displacement response was obtained for the hybrid system having constant axial load (Fig. 15). A comparison with test PT<sub>NC</sub>7 shows a reduction in total strength and lower bilinear stiffness due to the constant moment contribution at the column base with higher energy dissipation being provided by friction from the axial load control system.

The force-displacement hysteresis of tests PT7 and PT10 are overlain together in Figure 16 (left), both having constant axial load (7mm and 10mm fuse diameter respectively). While the response is very similar for the two systems, there is a slight increase in stiffness, strength and energy dissipation for test PT10 as expected.

Equivalent viscous damping ( $\zeta_{eq}$ ) was calculated for all the tests and illustrated in Figure 16 (right). As the dissipation content is increased the higher the equivalent viscous damping is perceived. A maximum of 14% of equivalent viscous damping is observed for test PT<sub>NC</sub>13.

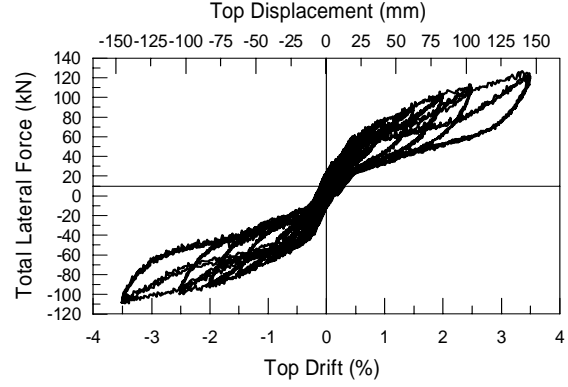


Figure 15. Hybrid system with external dissipators for TEST PT7: global hysteresis loop at 3.5 % drift.

Due to buckling of the dissipators between a lateral drift of 2% and of 2.5%, a reduction in the  $\zeta_{eq}$  is observed there after. The dissipators within test PT<sub>NC</sub>13 have greater anti-buckling resistance and thus no  $\zeta_{eq}$  degradation is observed. A comparison between the constant and variable load tests shows no significant differences for the  $\zeta_{eq}$ .

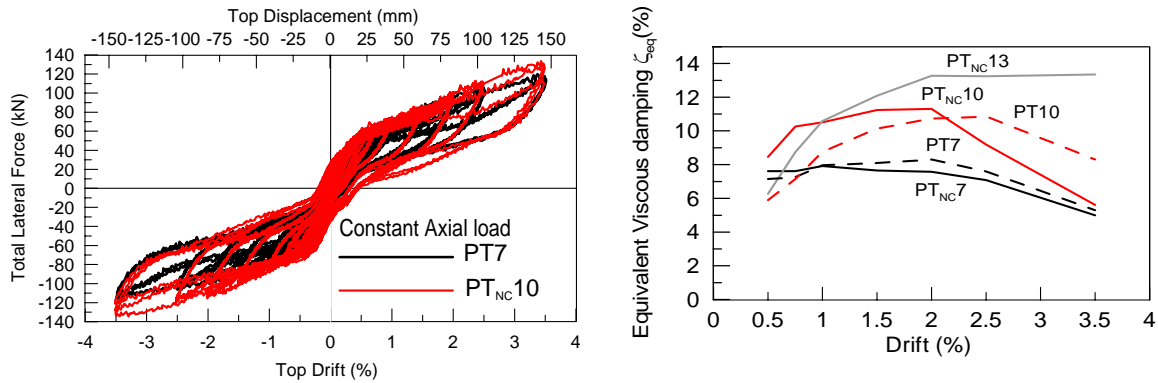


Figure 16. Comparison between varying or constant axial load and equivalent viscous damping.

## 5 ANALYTICAL-EXPERIMENTAL COMPARISON

Several different approaches are described in literature to model the connection of the precast concrete systems with different levels of complexity. Included are section analysis (Priestley and Tao 1993), finite element analysis (Kurama et al., 1999) and lumped plasticity models using moment-curvature/rotation responses (Pampanin et al., 2001) implemented via rotational springs. An overview of the different analytical models had been presented in Pampanin and Nishiyama (2002).

As the frame displaces, the gap at the beam-column interface opens and closes forming an infinite curvature at the critical section of the beam column joint. This violates strain compatibility and Bernoulli’s “plane sections remain plane” theory. Therefore, the use of a moment-rotation relationship is more appropriate when compared to traditional moment-curvature relationship.

A lumped plasticity modelling approach adopts non-linear inelastic rotational springs located in parallel at the rocking interface. The spring properties can be evaluated via a monotonic moment-rotation analysis which is evaluated based on a global member compatibility condition using the monolithic beam analogy principles (Pampanin et al., 2001, Palermo, 2004). The analysis allows each moment contribution (mild steel, post-tensioned tendons and axial load) to be isolated, defining their individual contributions and allowing individual spring properties to be defined.

Appropriate hysteretic rules are assigned to each spring property to correctly represent the inelastic behaviour at the beam-column joint (Figure 17). Elastic elements are used to represent the precast structural members as proposed in (Pampanin et al., 2001).

The unbonded post-tensioned tendon was model using a linear elastic rotational spring, while a second non-linear inelastic spring was used to represent the mild steel energy dissipation contribution: a number of options included a) Bi-linear inelastic, b) Ramberg-Osgood, and c) Dodd-Restrepo hysteresis.

As the dissipaters are displaced into net negative displacements and buckling is initiated the dissipater does not contribute to the energy dissipated in the system. However, the bearing effect onto the epoxy filled material increases the compression stiffness and strength as was previously explained and illustrated in the experimental results presented earlier (Figure 7). An additional compression-only moment-rotational spring is added at the same location as the dissipaters such that the combined stiffness and strength between the two springs in parallel represents the observed behaviour during testing of the dissipater elements.

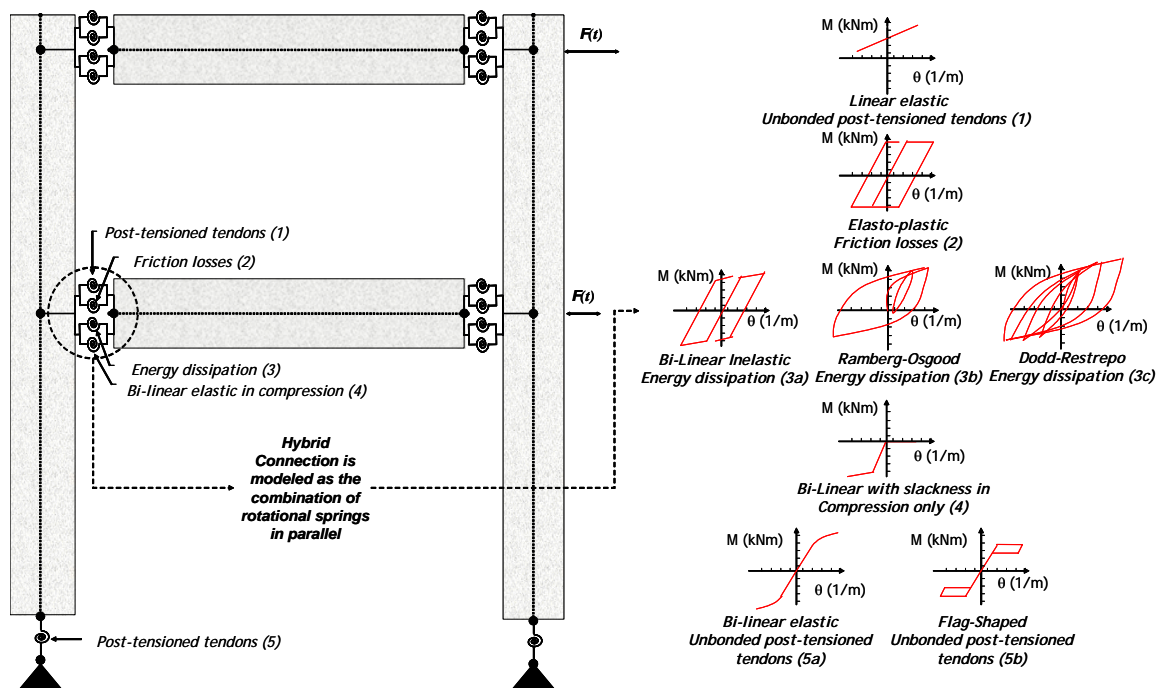


Figure 17. Analytical-experimental comparison using lumped plasticity model.

Friction forces occurring between the tendons and the plastic ducts were also considered. The friction force is determined using fundamental prestress theory where the vertical force components from the post-tensioned tendon are multiplied by the code recommendations for friction coefficients (between 0.05 and 0.15). A simple moment rotational spring was implemented with an elasto-plastic hysteresis rule considering a high initial stiffness where the yield moment corresponded to the friction force in each tendon multiplied by the individual internal lever arms.

A simple bi-linear elastic hysteresis rule was adopted at the column base to model the axial force moment contribution due to the post-tensioned tendons. A flag-Shaped hysteresis rule was adopted at the column base for the constant axial load system which accounted for the additional energy lost due to the axial load control system

The non-linear finite element program Ruaumoko2D (Carr, 2006) was used to model the series of experimental tests adopting each of the moment-rotation springs above. The recorded lateral force time history during testing was used as the input loading history for the model at each floor.

Given the simple hysteresis rules adopted, Figure 18 illustrates how the global hysteresis response is accurately represented for tests  $PT_{NC}$  and  $PT_{NC7}$  (Fig. 18 left and right respectively). It can be seen the

model can reproduce the experimental results with reasonable accuracy despite of the analytical validation of test  $PT_{NC}$  was simpler than adding energy dissipation (test  $PT_{NC7}$ ) due to the complexity of the dissipation behaviour in compression.

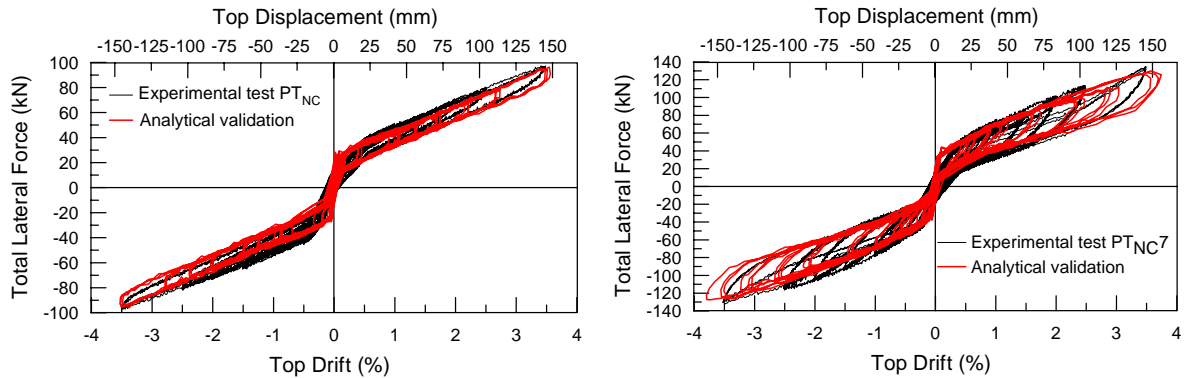


**Figure 18. Analytical-experimental comparison: Force displacement response of test  $PT_{NC}$  (left) and  $PT_{NC7}$  (right).**

Analytical experimental validation comparisons between the unbonded post-tensioned tendons and the energy dissipation, moment rotation are shown in figure 19 left-and right respectively. The linear elastic behaviour of the post-tensioned tendons was combined with the bi-linear inelastic hysteresis representing the friction in the tendons (Fig. 19-left). A small discount of the tendon forces is required to do not account for higher strength of forces in the model due to the friction force contribution.

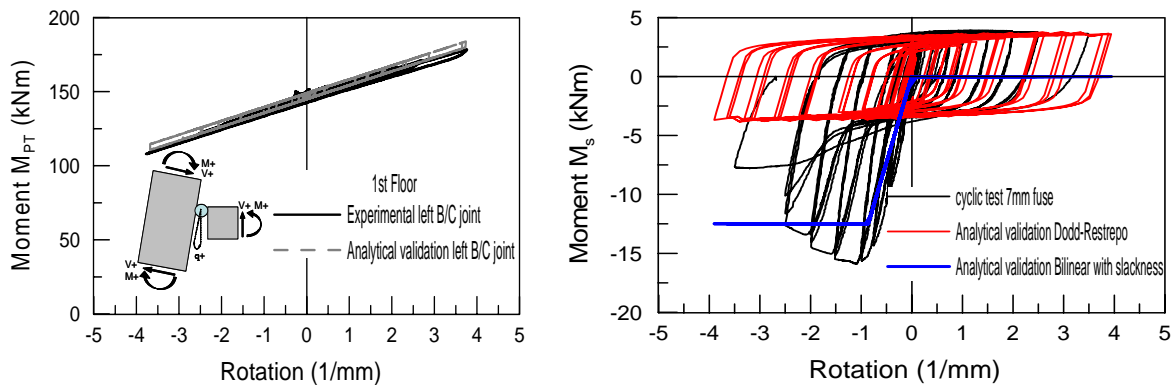


**Figure 19. Analytical-experimental comparison: B/C joint unbonded post-tensioned tendon (left) and mild steel dissipation (right) moment rotation behaviours.**

Modelling the energy dissipater (fig. 19-right) required a proper understanding of the response. Different hysteresis rules were adopted in order to capture the real behaviour of the dissipater. Non-linear inelastic rules such as Ramberg-Osgood and Dodd-Restrepo were implemented. The bi-linear inelastic hysteresis rule was not appropriate for the model as Bauschinger effects could not be captured, meanwhile the Ramberg-Osgood hysteresis rule requires iteration on the power factor to obtain the desire monotonic moment-rotation response. The Dodd-Restrepo hysteresis rule is more appropriate in modelling the dissipaters as proper material non-linearity and Bauschinger effects are accounted for.

Figure 19-right shows the response using the Dodd-Restrepo hysteresis rule. An additional bilinear, compression-only spring is also presented to model the bearing contact in compression. The calculation of the stiffness and maximum yield moment is difficult to predict due to the unknown epoxy properties and the possible contribution of the outer steel tube. The stiffness and strength was simply calibrated from cyclic steel testing of the dissipaters.

The moment rotation response at the column foundation was modelled using a non-linear elastic

hysteresis rule at the base of the frame. Figure 20 illustrates the analytical experimental-validation agreement considering constant or variable axial load. The experimental tests having variable axial load (PT<sub>NC</sub>, PT<sub>NC7</sub> and PT<sub>NC10</sub>) were modelled using a bi-linear elastic hysteresis (Fig. 20-left).

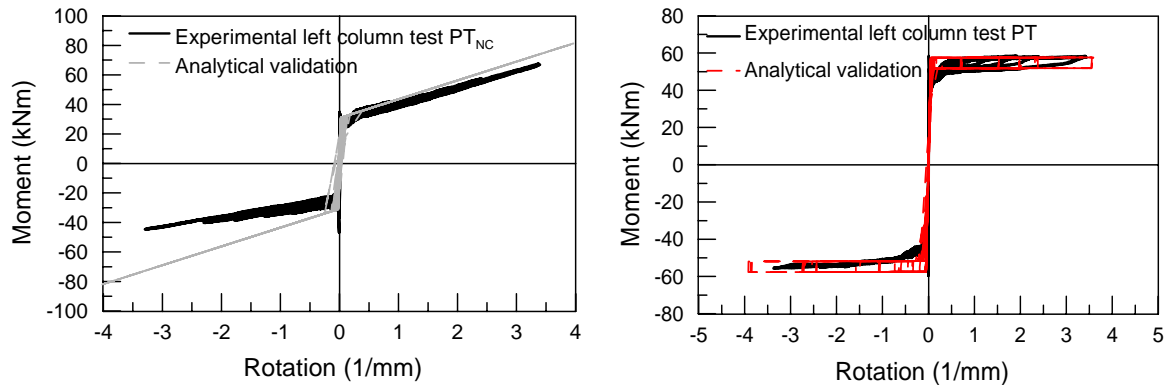


**Figure 20. Analytical-experimental comparison: Column-foundation connection test PT<sub>NC</sub> (left) and test PT (right) moment rotation behaviours.**

Meanwhile, the constant axial load tests (PT, PT7 and PT10) were modelled using a flag-shaped hysteresis behaviour (Fig. 20-right). Energy dissipation was considered in the hysteresis model to account for the additional energy loss due to the axial load setup and control.

## 6 CONCLUSIONS

The implementation and experimental validation of a non-tearing-floor solution concept for precast jointed ductile connections, relying on unbonded post-tensioning techniques and the use of external dissipation has been presented with very satisfactory results.

Both experimental and analytical comparisons of the results on quasi-static cyclic testing of a two-story, one bay precast frame, implementing the proposed non-tearing floor solution, provide satisfactory confirmation that the effects associated with beam elongation are eliminated, thus significantly reducing the expected damage in the floor.

It was demonstrated that the global flag-shape behaviour can be controlled either by assuming the only contribution of the self weight of the structure or adding unbonded post-tensioned tendons such that full re-centring can be achieved by the ratio between axial force and dissipation.

Although the innovative floor solution presented herein significantly reduces the effects of beam elongation, further refinements will include improvements in the energy dissipater devices as well as to guarantee the actual constructability (tolerances issues)

Validation of the results using simple moment rotational springs has provided good agreement with the experimental results. A series of numerical investigations are under-preparation to provide further confirmation of the enhanced global seismic behaviour and implemented for design purposes.

A large scale test on a 3-D super-assembly is under-preparation to provide further experimental confirmation of the enhanced global seismic behaviour of the non-tearing floor concept with the combination of different connection arrangements.

## ACKNOWLEDGEMENTS

The financial support provided by the NZ Foundation of Research, Science and Technology (“Future Building System” research project) is greatly appreciated.

## REFERENCES

- ACI T1.1-01 & ACI T1.1R-01. 2001 Acceptance Criteria for Moment Frames Based on Structural Testing (T1.1-01) and Commentary (T1.1R-01). *ACI Innovation Task Group 1 and Collaborators*.
- Amaris, A. Pampanin, S., Bull, D & Carr, A. 2007. Development of a Non-tearing Floor Solution for Jointed Precast Frame Systems. *Proceedings of The New Zealand Society of Earthquake Engineering Annual Conference*, Parmerston North, New Zealand.
- Carr, A. 2006. RUAUMOKO program for Inelastic Dynamic Analysis – User Manual. Department of Civil Engineering, University of Canterbury, Christchurch, New Zealand.
- Douglas, K.T. 1992. Elongation in Reinforced Concrete Frames. PhD Thesis, Department of Civil Engineering, University of Auckland.
- Fenwick, R.C. and Fong, A. 1979. The Behaviour of Reinforced Concrete beams Under Cyclic Loading. Research Report, Department of Civil Engineering, University of Auckland.
- Fenwick, R. C. and Megget, L. M. 1993. Elongation and Load Deflection Characteristics of Reinforced Concrete Members containing Plastic Hinges. *Bulletin of the New Zealand National Society for Earthquake Engineering*, 26 (1). 28-41.
- Kurama, Y., Sause, R., Pessiki, S. And Lu, L.-W. 1999. Lateral load behaviour an seismic design of unbonded post-tensioned precast concrete walls. *ACI structural Journal*. 96(4). 622-632.
- Nakaki, S.E., Stanton, J. F., Sritharan S. 1999. An Overview of the Presss Five-Story Precast Test Building. *PCI Journal*, 44 (2). 26-39.
- Matthews, J., D. Bull, and Mander J. 2003. Hollowcore floor slab performance following a severe earthquake. Concrete Structures in Seismic Regions. Proceeding of the First fib Symposium. Athens, Greece.
- NZS3101:2006. 2006. Concrete Structures Standard. Standards New Zealand, Wellington, New Zealand.
- Ohkubo, M., Hamamoto, T. 2004. Developing Reinforced Concrete Slotted Beam Structures to Reduce Earthquake Damage and to Enhance Seismic Structural Performance. Proceedings of the 13<sup>th</sup> World conference on Earthquake Engineering. Vancouver, Canada
- Palermo, A. 2004. The use of controlled rocking in the Seismic Design of Bridges. Ph.D. dissertation, Politecnico di Milano, Milano, Italy.
- Pampanin S., Priestley N., and Sritharan S. 2001. Analytical Modelling of the Seismic Behaviour of Precast Concrete Frames Designed with Ductile Connections. *Journal of Earthquake Engineering*. 5 (3). Imperial College Press. 329-367.
- Pampanin S. and Nishiyama M. 2002. Critical aspects in modelling the seismic behaviour of precast/prestress concrete building connection and systems. Proceeding of the First fib Congress. Osaka, Japan
- Pampanin S., Amaris A., Akguzel U., and Palermo A. 2006. Experimental Investigations on High-Performance Jointed Ductile Connections for Precast Frames. Proceedings of the First European Conference on Earthquake Engineering and Seismology. Geneva, Switzerland.
- Pincheira, J.A., Oliva M. G. and Zheng W. Behaviour of Double-tee Flange Connectors Subjected to In-plate Monotonic and Reversed Cyclic Loads. *PCI Journal*. 50 (6). 1-24.
- Priestley MJN. 1991. Overview of the PRESSS Research Programme. *PCI Journal*. 36 (4), 50-57.
- Priestley, M.J.N. and Tao, J. R. 1993. Seismic Response Of Precast Prestressed Concrete Frames With Partially Debonded Tendons. *PCI Journal*. 38 (1). 58-69.
- Priestley, M.J.N. 1996. The PRESSS Program-Current Status and Proposed Plans for Phase III. *PCI Journal*. 41(2). 22-40.
- Priestley, M.J.N., Sritharan, S., Conley, J.R. and Pampanin, S. 1999. Preliminary Results and Conclusions From the PRESSS Five-Storey Precast Concrete Test Building. *PCI Journal*. 44 (6). 42-67
- Priestley, M.J.N. 2002. Direct Displacement-Based Design of Precast/Prestressed Concrete Buildings. *PCI Journal*. 47 (6). 66-78